Graphene oxide-polysulfone hollow fibers membranes with synergic ultrafiltration and adsorption for enhanced drinking water treatment

Journal of Membrane Science 658 (2022) 120707

Contents lists available at ScienceDirect

Journal of Membrane Science

journal homepage: www.elsevier.com/locate/memsci

Graphene oxide-polysulfone hollow fibers membranes with synergic ultrafiltration and adsorption for enhanced drinking water treatment

Massimo Zambianchi [a,1], Sara Khaliha [a,1], Antonio Bianchi [a,1], Francesca Tunioli [a], Alessandro Kovtun [a], Maria Luisa Navacchia [a], Anastasio Salatino [b], Zhenyuan Xia [c], Elena Briñas [d], Ester Vázquez [d,e], Davide Paci [f], Vincenzo Palermo [a], Letizia Bocchi [f], Barbara Casentini [b], Manuela Melucci [a,*]

[a] Consiglio Nazionale Delle Ricerche, Institute for Organic Synthesis and Photoreactivity (CNR-ISOF), Via Piero Gobetti 101, 40129, Bologna, BO, Italy
[b] Consiglio Nazionale Delle Ricerche, Institute for Water Research (CNR-IRSA), Via Del Mulino, 20861, Roma, RM, Italy
[c] Industrial and Materials Science, Chalmers University of Technology, 41258, Göteborg, Sweden
[d] Regional Institute of Applied Scientific Research (IRICA), UCLM, 13071, Ciudad Real, Spain
[e] Department of Organic Chemistry, Faculty of Science and Chemistry Technologies, University of Castilla-La Mancha (UCLM), 13071, Ciudad Real, Spain
[f] Medica Spa, Via Degli Artigiani 7, 41036, Medolla, MO, Italy

ARTICLE INFO

Keywords:
Graphene oxide
Polysulfone hollow fiber
Adsorptive-ultrafiltration membranes
Drinking water treatment
Emerging contaminants

ABSTRACT

Polysulfone-graphene oxide hollow fiber membranes (PSU-GO HFs) with simultaneous adsorption and ultrafiltration capabilities are herein described and proposed for enhanced and simplified Point-of-Use (POU) drinking water purification. The PSU-GO HFs were prepared by phase inversion extrusion by a customized semi-industrial plant and their morphology, surface properties, and porosity were investigated by combined Scanning Electron Microscopy (SEM), contact angle and Raman confocal microscopy, in relation to different GO:PSU ratios (1–5% w/w GO vs PSU) and to the final adsorption-ultrafiltration properties. Filtration modules of PSU-GO HFs of filtering surface (FS) in the range 0,015–0,28 m^2 showed same ultrafiltration capability of PSU-HF standard filters. Synergic adsorption properties were demonstrated by studying the adsorption maximum capacity of ciprofloxacin antibiotic (CIPRO) vs GO ratio in dead end in-out configuration, the standard configuration used for PSU HFs commercial modules. Loading of 3,5% GO vs PSU was selected as case study, representing the best compromise between performance and GO nanofiller amount. Heavy metals (Pb, Cu and Cr(III)) and polyfluoroalkyl substances (PFAS) removal capabilities from tap water were competitive and in some cases outperformed Granular Activated Carbon (GAC), the standard industrial sorbent. Ciprofloxacin removal from tap water was also under real operational conditions. Moreover, release of GO from working PSU-GO modules was excluded by Surface Enhanced Raman Spectroscopy (SERS) analysis of treated water having the state-of-the-art limit of quantification of 0.1 μg/L for GO nanosheets.

1. Introduction

Polysulfone (PSU) porous membranes are well-known and used membranes for micro and ultrafiltration for hemodialysis and water disinfection purposes [1–4]. Their wide range of applications relies on the structure versatility of such membranes, with morphology and porosity that can be tuned by the choice of several parameters including processing solvent/non solvent, coagulation temperature, casting solution composition and humidity [5–7]. In recent years, aiming at membranes with enhanced mechanical properties, biofouling resistance and multifunctionality, doping of PSU membranes (mainly flat membranes) with nanomaterials have been widely investigated [8].

Carbon-based nanomaterials such as carbon nanotubes (CNT), nanofibers and graphene-reinforced membranes have been fabricated by phase inversion processes adapted to integrate such nanomaterials [9]. It has been shown that doping of PSU with carbon nanotubes of different structure (single, multiwalled) and functionalization (i.e. amine, azide, carboxylic groups) increases water permeability (up to ~600 $Lm^{-2}h^{-1}$)

* Corresponding author.
E-mail address: manuela.melucci@isof.cnr.it (M. Melucci).
[1] These authors contributed equally to this work.

https://doi.org/10.1016/j.memsci.2022.120707
Received 9 April 2022; Received in revised form 20 May 2022; Accepted 4 June 2022
Available online 7 June 2022

[10], improves tensile strength and modulus, increases materials crystallinity and thermostability [11] and enhanced rejection of NaCl solution [12]. With the advent of graphene 2D materials, having higher processability and lower costs than CNT, graphene doped membranes have been also realized [13,14] and have shown improved thermal and mechanical properties [15,16], ion exchange capability [17] and arsenate rejection capability (just to mention few) [18], than undoped analogues.

Adsorption properties were observed for these membranes [19,20]. For instance Badrinezhad et al. demonstrated methylene blue adsorption from water with removal efficiency of about 80% by 0,75% doped PSU membranes [21] and desorption of about 40% which was lower that than observed in graphene free membranes. Some of us, reported the fabrication of PSU-GO adsorptive membranes with 5% in weight of GO content and demonstrated the ability of this membranes to adsorb selected emerging contaminants (ECs) in mixture in tap water with significant enhancement of removal of hydrophilic molecules including ofloxacin antibiotic, carbamazepine and diclofenac [22].

On this line, here we report the fabrication of PSU hollow fiber (PSU-HFs) membranes through an ad hoc developed industrial pilot plants (Medica spa, production capacity 200,000 Km/yr) doped with GO at different loadings (PSU-GO HFs). We investigated the structural, filtration and adsorption properties of modules realized by the newly developed HFs aimed at their exploitation for the fabrication of multifunctional modules for point-of-use (POU) drinking water treatment.

POU drinking water treatment systems are installed on the water supply lines ahead of water taps, and/or dispensers to provide on-site water purification. A wide range of POU technologies have emerged in recent years including adsorption membrane filtration and disinfection that are combined in a specific sequence to form a POU system. These systems are exploited to adjust water taste and odour and are expected to remove hazardous contaminants such as ECs [23–28] not completely removed during drinking water treatment such as perfluoroalkyl chain substances (PFASs) [29–36].

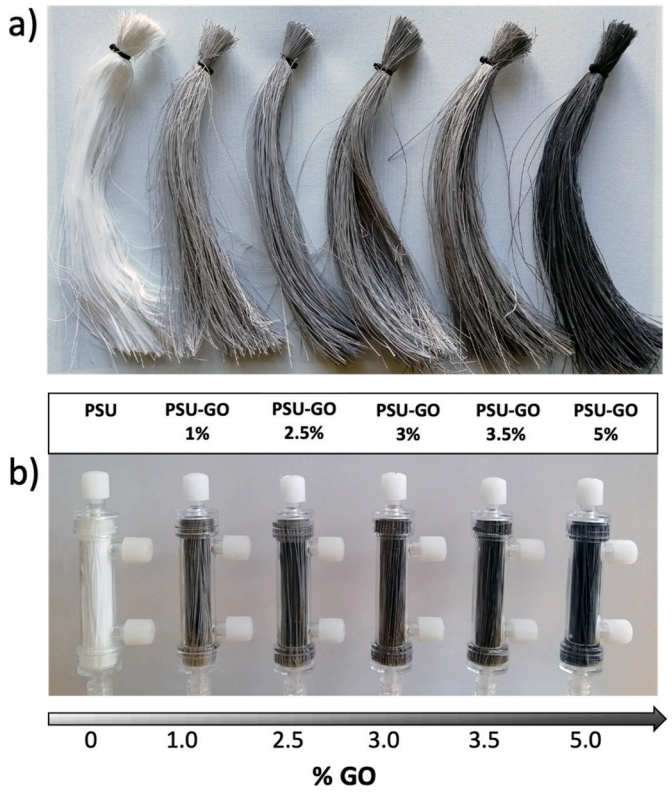

Fig. 1. a) PSU HFs and b) filtration modules, with different amounts of GO (w/w). From left to right: pristine PSU; PSU-GO 1%; PSU-GO 2.5%; PSU-GO 3%; PSU-GO 3.5%; PSU-GO 5%. Details of fibers spinning, and modules fabrication are described in ESI (Fig. S1). Cartridge size are 6.5 cm length, 1.5 cm diameter, 4.5 mL dead volume.

Polysulfone hollow fiber (PSU-HFs) membranes consist of hollow fibers with surface pores and macrovoids of porosity in the range 5–100 nm that have been recently introduced in the POU water purification market for water disinfection, i.e. removal of bacteria, viruses and endotoxins capability. PSU-HFs modules are exploited as last treatment step after adsorption and/or ion exchange and/or reverse osmosis steps to remove pathogens [37,38]. Aiming at simplified and more efficient POU systems [39], here we propose adsorptive PSU-GO HFs based modules for combined ultrafiltration and adsorption of different water pollutants, both organics and heavy metals. Previous studied on PSU-HFs doped with carbon nanoparticles and prepared by phase inversion DMF→water showed adsorptive capability toward benzene, phenol and toluene from aqueous solution [40] with adsorption capacity (q_{max}) of the membranes increasing with carbon nanoparticle concentration in the range 50–60 mg/g. Zahri et al. [41] reported PSU-graphene oxide hollow fiber membranes prepared by phase inversion from a mixture DMAC, THF and EtOH to water and demonstrated gas separation properties with CO_2/N_2 and CO_2/CH_4 selectivity enhancement by 158% and 74% respectively with respect to neat PSU membranes. More recently, Sainath et al. further enhance the CO_2/CH_4 gas separation performance of PSU-GO HFs by zeolitic imidazolate nanoparticles inclusion [42].

However, at the best of our knowledge no examples of PSU-GO HFs for combined adsorption and ultrafiltration for the removal of pollutants in mixture in tap water have been reported. Here, we consider selected organic and heavy metal contaminants of concern recently revised in the drinking water directive EU 2020/2184 [43], including perfluoroalkyl substances (PFASs) [29–34] Pb and Cr [44,45] and studied their adsorptive removal by the newly developed PSU-GO HF modules. Moreover, to evaluate safe use of the proposed filters for drinking water filtration, we tested the release of GO nanosheets from such modules through Surface Enhanced Raman Spectroscopy (SERS) method, allowing state of the art limit of quantification of GO in water down to 0.1 ppb.

2. Experimental part

2.1. Materials

GO powder was purchased from Abalonyx (AS, Norway, now Layer One, Aker) and used without further purification (graphene oxide dry powder <35 mesh, product code 1.8, XPS: O/C ratio 0.39 ± 0.01, C 70.1 ± 0.9%, O 27.2 ± 0.9%, N 0.2 ± 0.1%, S 1.0 ± 0.1%, Si 0.8 ± 0.1%, Cl 0.7 ± 0.1%, Mn below 0.1%). Standard PSU HFs (Medisulfone®) and PSU Ultrafiltration modules were provided by Medica Spa.

2.2. Porosity

PSU HFs and PSU-GO 3.5% HFs have been analyzed for pore size and pore distribution through liquid-liquid-displacement-porometer (LLDP), Poroliq TM1000 (Porometer, Germany-Belgium). PSU HFs porosity were measured after spinning without glycerinization, since glycerin impairs the porometer measurement. PSU-GO 3.5% HFs were analyzed after mild glycerinization, extensive water washing and air-drying at room temperature, to remove any glycerin residual. Fibers to be analyzed by LLDP were prepared by horizontally placing one or more hollow fibers into the holder and sealing with a bicomponent glue the fibers' edges; measurement occurred in out-in modality. The isobutanol saturated with water was the wetting liquid and the water saturated with butanol was the displacement liquid.

2.3. HF spinning and module assembling

The dope solution is prepared adding PSU granules to a GO solution in NMP, obtained after 24–36 h of sonication, at room temperature (25 °C). PSU is mixed with the GO solution (ratio 1 → 5% w/w PSU/GO, polymer concentration range 10–20% PSU-GO/NMP), alternating propeller immersion mixing and sonication, while viscosity is checked periodically. The resulting dope solution is extruded with a lab scale benchtop spinning plant, with a maximum dope solution capacity of 3 kg at room temperature (Hollow fibers spinning plant is shown in Fig. S1, ESI). During extrusion in the spinneret, the dope solution enters in contact with a precipitation solution composed of water and NMP. The PSU-GO HFs then freely fall in a coagulation bath, are collected by a bobbin system, moved into a washing bath, and finally collected onto a collection wheel. Fibers are stocked in bundles and then kept in water for solvent extraction and glycerinization, and ultimately dried at open air. 1 kg of material corresponds approximately to 20 km of fibers.

Lab-scale modules of standard PSU Medisulfone® and PSU-GO HFs were prepared. Small bundles of closed fibers are obtained cutting the dried stocked bundles with a hot wire. Fibers are then potted in polyurethane resin at the edges inside a module scaffold and then centrifuged. The potting is ultimately cut (to open the fibers) and headers were welded.

Filtering surface (FS) of the modules was 0,025 m^2 (standard PSU HFs) or 0.015 m^2 (PSU-GO HFs) and they were assembled into a cartridge of 5 mL dead volume.

For characterization at tap POU, modules with U-shaped fibers were prepared with FS 0.28 m^2; U-shaped modules can be directly connected to the tap, working with tap water pressure (3 bar; mean flow rate 5 L/min).

2.4. Ciprofloxacin adsorption experiments

The adsorption capacity of PSU-GO HFs containing different GO loadings (Fig. 1) was tested under dynamic conditions by filtering tap water spiked with ciprofloxacin. In a typical experiment, 5 mg/L CIPRO tap water solution was filtered in dead end in-out transmembrane modality on PSU-GO HFs module at a constant flow of 5 mL/min. Fractions each 200 mL were collected and analyzed by UV–Vis analysis (Agilent Cary 3500) to determine CIPRO concentration. The filtration experiments were carried out until the removal was below 2%. The experiments were repeated in triple by using new modules for each repetition.

2.5. Cut-off determination by dextrans filtration

Fluorescent dextrans at different molecular weight (MW) were used as tracers for cut-off determination. Fluorescein isothiocyanate dextran 4 kDa, 10 kDa, 20 kDa, 40 kDa, 70 kDa were purchased from Merck. A solution of each tracer in *N*-propyl-gallate was prepared at a concentration of 5 mg/mL. Lab-scale modules of PSU and PSU-GO 3.5% HFs were tested, (three modules for each tracer). The modules were prerinsed with water and the tracer solution was filtrated in dead end in-out modality at constant pressure. The filtrate was collected in sequential fraction of 500 μL volume each. A total of 12–14 fractions were collected for each module. Samples were analyzed by a fluorometer (Fluoroskan, ThermoFisher Scientific) at the excitation wavelength of 484 nm and emission wavelength of 538 nm. Experiments were repeated in triple by using each time a new module.

2.6. PFASs removal experiments and analysis

Tap water spiked with a mixture of fourteen PFASs C_3–C_{13} was prepared and filtered (dead end, in-out) at 5 mL/min using a Cole-Parmer Masterflex® peristaltic pump on the selected PSU HFs, PSU-GO 3.5% HFs and GAC modules, previously washed with 2 L of MilliQ water. GAC was tested for comparison. The concentration of each contaminant was 0.5 μg/L in a total volume of 1 L. The concentration of PFASs in filtered water was analyzed by UPLC-MS/MS (Waters Acquity, UPLC BEH C18 analytical column, details in ESI).

2.7. Heavy metals removal experiments and analysis

Mineral water spiked with a mix of heavy metals and metalloids (Pb, Cu, Cd, Ni, Cr(III), As(V), V and U) at a final concentration of 100 μg/L each was prepared starting from individual 1 g/L stock solutions (ICP-MS standards, VWR). Spiked mineral water was filtered on selected modules (PSU HFs, PSU-GO 3.5% HFs and GAC), previously washed with 1 L of MilliQ water. Flow was set at 5 mL/min and 3 L of water were treated, then flow was incremented to 40 mL/min and two more liters treated for a preliminary evaluation of performance under different flow conditions of the selected modules. Samples were collected every 200 mL. Each fraction was immediately acidified with 1% HNO_3 Suprapur (Sigma-Aldrich) and solutions were analyzed by ICP-OES (Model 5800, Agilent).

At the end of the filtration experiment, the mobility of adsorbed contaminants was tested by passing three fractions of 50 mL MilliQ water at 20 mL/min in-out mode, and two more fractions of 50 mL in reverse out-in flow. Concentration was measured as described above and percentage of release respect to total adsorbed was calculated. Module filling material weight was 0.2, 0.26 and 1.5 g for PSU HFs, PSU-GO 3.5% HFs and GAC, respectively. All tests were carried out in duplicate and reported as mean value with standard deviation.

2.8. Potability of filtered water

Chemical and biological parameters included in the Italian D.Lgs 31/01 (implementation of 98/83/EU Directive) were tested in tap water before and after in-out filtration through PSU-GO 5% module with U-shaped fibers of FS 0.28 m^2 at 5 L/min, total volume 100 L.

2.9. GO release tests by SERS

PSU HFs and PSU-GO 3.5% HFs modules were washed with 2 L of hot MilliQ water (80 °C) in dead end in-out configuration at 50 mL/min using a Cole-Parmer Masterflex® peristaltic pump, to remove glycerin. After that, 1 L of tap water was filtered in-out modality at a flow of 250 mL/min in PSU HFs, sampling every 250 mL. Thereafter, 500 mL, collected from the previous fractions, were recirculated for 2 h at 250 mL/min. The flow used was significantly higher than the maximum one that the module is supposed to ensure to guarantee porosity and filtration capacity (i.e. max flow 50 mL/min). This flow may cause mechanical stress of the hollow fibers, with possible release of GO from the fibers. Same procedure was performed on PSU-GO HFs. Samples were analyzed using surface-enhanced Raman spectroscopy (SERS), following a previously described protocol [46]. Analytical features of the method for the determination of GO nanosheets in water are described in ESI (Table S7, Figs. S13–S16, ESI). The calibration curve shown in the inset of Fig. 10 was built using the intensity of the D peak, as analytical signal, for the concentration range 0.1–10 μg/L. The practical limit of quantification (P-LOQ), which is defined as the minimum level at which GO can be measured in water samples with accuracy higher of 80% and relative standard deviation (RSD) lower than 10%, was 0.1 ppb.

Additionally, to confirm that our methodology can detect GO release from the PSU-GO fibers, previously used PSU HFs modules and both used and new PSU-GO HFs modules were opened with a hacksaw (ESI, Fig. S14). Fibers extracted from the modules were cut and dried in a desiccator for 72 h. Subsequently, a known weight of fibers was added to 20 mL of deionized water and overstressed through sonication for 30 min in an ultrasonic bath. Three different weights of fibers were tested using three SERS substrates for each weight (ESI, Table S8).

Table 1
Diameters of through-pores (nm) obtained by using LLDP.

	Small pore size	Mean Flow Pore	Maximum pore size
PSU	6.2 ±0.3	6.4 ±0.4	6.5 ±0.3
PSU-GO 3.5%	11 ±1	13 ±2	22 ±6

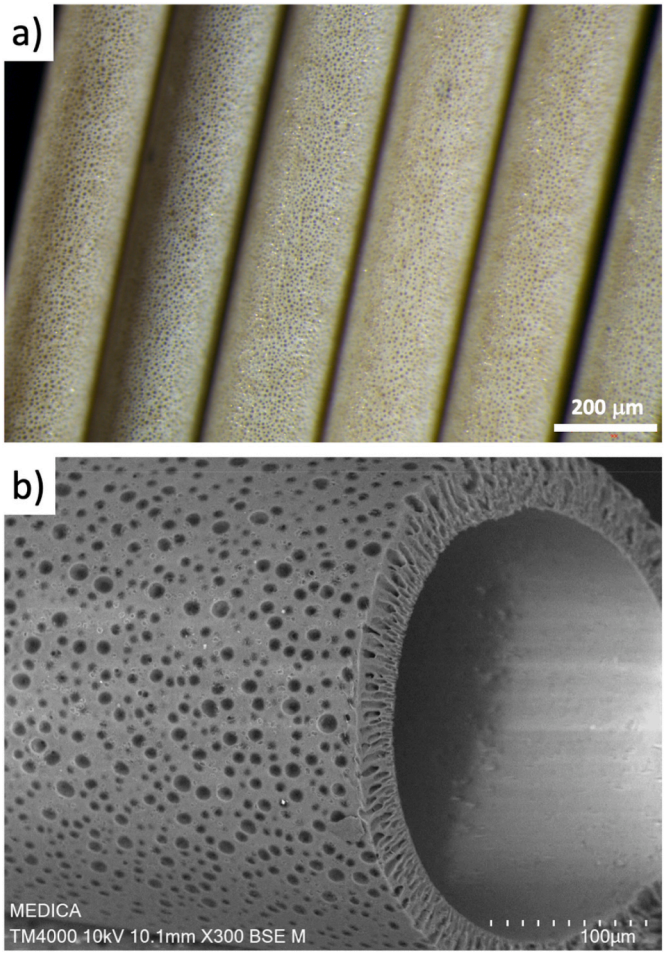

Fig. 2. PSU-GO HFs morphology. a) Optical microscopy image of fibers, b) HF wall and section.

3. Results and discussion

3.1. PSU-GO HFs modules fabrication and characterization

Hollow fibers of PSU-GO at 1%, 2.5%, 3%, 3.5% and 5% w/w (GO: PSU) were obtained by phase inversion procedure (NMP→water) of a GO:PSU casting solution (PSU/NMP 10–20% w/w, PSU/GO 1–5% w/w) at room temperature, through a pilot spinning line, according to the protocol described in materials and method and by using the pre-industrial pilot line shown in Fig. S1. The membranes were then assembled in prototype modules (details in materials and method section) of filtering surface (FS) 0.015 m^2 that were then used for the following performance tests. The maximum flow rate acceptable for these cartridges was about 100 mL/min. Membranes and corresponding modules are shown in Fig. 1.

The pore average size of PSU and PSU-GO HFs were analyzed by porometer and the pore distribution through LLDP (Liquid-Liquid-Displacement-Porometer, details in materials and methods). The size of through-pores of PSU and PSU-GO fibres was considered as the MFP (Mean Flow Pore Size) which represents the pore range with an amount of 50% of the total flow (point of intersection of LLDP- and Half-Perm-Curve).

Table 1 summarize porosity data (see also Table S1, ESI). PSU-GO HFs showed average pore size of 13 nm, i.e. higher than that determined for standard PSU HFs (6 nm), this being likely due to the slightly different extrusion conditions exploited for PSU-GO spinning.

The morphology of PSU-GO fibers resemble that of the pristine PSU HFs with wall section thickness of about 50 µm, lume diameter of 250–300 µm and outer porosity of 5–10 µm Fig. 2 (and Fig. S2, ESI). Fig. 2 shows the observe general morphology of PSU-HFs observed by optical microscopy under ambient light and the detail of a single fiber observed by SEM.

The cross-section SEM images of PSU-GO HFs as a function of the GO loadings, at 1%, 3.5% and 5% loading are instead shown in Fig. 3 and Fig. S2 ESI. PSU-GO HFs show the typical hollow fiber structure, with extended finger-like pores and a thin sponge-like layer beneath it. An average wall thickness of ca. 45 ± 5 µm and inner diameter of ca. 220 ± 20 µm was observed for all the samples together with a slight increase in the micro-void size is observed on increasing GO loading. Some large GO flakes can be seen exposed at the outer surface of the pores (Fig. 3f, representative SEM image of PSU-GO 1%) in accordance with the contact angle measurements (Fig. S3, ESI), showing a decrease from 60.1 ±4.1° for PSU to 53.1±2.1° for PSU-GO 3.5%, indicating a slight enhancement of the surface hydrophilicity.

Raman spectra of GO and PSU-GO HFs are showed in Fig. 4. The spectrum of PSU showed main peaks located at around 790, 1146, 1584, 1605, and 3068 cm^{-1}, correlated to the asymmetric C–S–C, asymmetric C–O–C vibration, aromatic ring chain vibration, and C–H vibration, respectively. The broad peak at around 2900 cm^{-1}, can be ascribed to the PSU methyl bonds. The Raman spectrum of GO showed two characteristic peaks at 1350 and 1596 cm^{-1} (Fig. 4a), corresponding to the D band (defects or disorders) and G band (pristine sp^2 carbon atoms) of GO. No overlap between the D band from GO and other characteristic peaks of PSU were observed this allowing the identification of GO distribution on PSU-GO composites by Raman mapping.

Raman mapping and depth profiling techniques are shown in Fig. 4b and fig. S4 (ESI). All tested PSU-GO samples, including 1%, 3.5% and 5% GO loading amount, showed GO almost homogeneous distribution inside the hollow fiber section. As expected, PSU-GO 5% revealed the highest D peak intensity (5×10^4 CCD cts). Meanwhile, GO flakes on PSU-GO 3.5% showed the best integration with the finger-like PSU matrix structure, according to the D peak distribution of GO from the relative z-stack imaging (Fig. 4b).

3.2. Tailoring of GO loading in PSU-GO HFs

Ciprofloxacin (CIPRO), a fluoroquinolone antibiotic, is strongly adsorbed by GO [47] but it is not removed by PSU HFs, thus we here exploited CIPRO removal from water to study its adsorption as a function of GO loading amount in order to optimize the hollow fibers composition. Tap water spiked with CIPRO was filtered through modules of PSU-GO HFs in Fig. 5a, dead-end transmembrane modality (in-out), at low flow rate (5 mL/min) until breakthrough was reached (about 3L filtered). CIPRO spike at 5 mg/L was chosen to enable fast detection by UV, the low flow rate was selected to reach the highest contact time allowed in flow experiments and establish the highest removal capacity of the modules. Three independent modules were used for each loading curve experiment. We estimated the maximum adsorption capacity (Qmax) as milligrams of CIPRO removed per gram of composite by the plateau of the loading curves (PSU-GO, Fig. S5, ESI). As shown by Fig. 5b the performances were independent from the initial concentration of CIPRO in the range 0.5–5 mg/L. The overall trend of adsorption capacity Qmax on increasing GO doping amount is shown in Fig. 4c, with Qmax increasing from 0.25 mg/g to about 6 mg/g from PSU HFs (0% GO) to PSU-GO 5% HFs. No significant advantage was observed by increasing GO amount from 3.5% to 5%, this highlighting PSU-GO

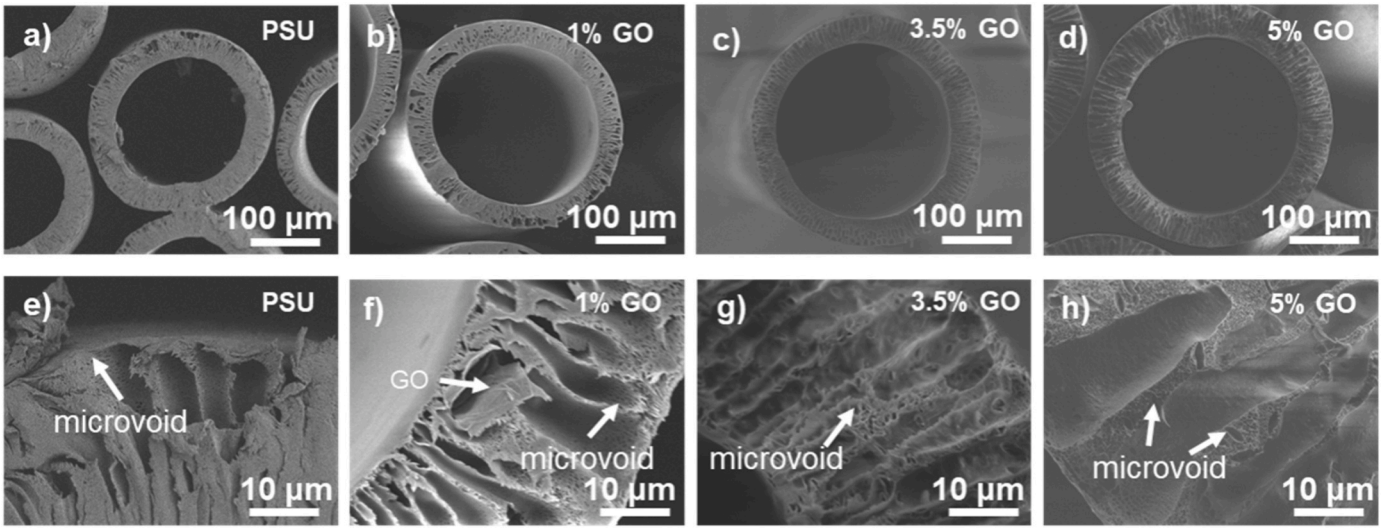

Fig. 3. Low and high magnification SEM cross-section images of a,e) bare PSU, b,f) PSU-GO 1%, c,g) PSU-GO 3.5%, d,h) PSU-GO 5% HFs.

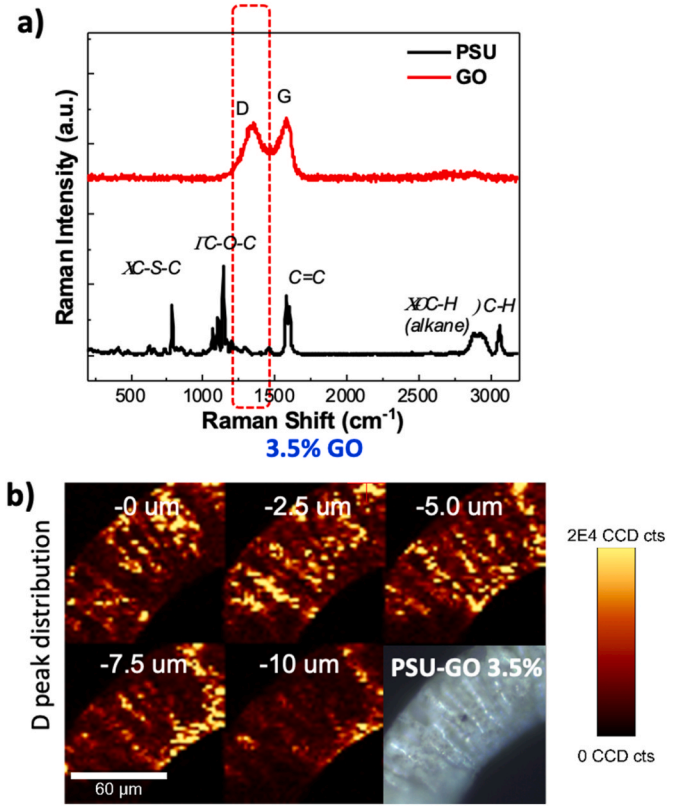

Fig. 4. a) Raman spectra of GO and PSU; b) Z stack of Raman maps and the relative optical image of PSU-GO 3.5% HFs, constructed by mapping the D-band region.

3.5% as the best compromise between performance and costs, mainly affected by GO doping amount.

The maximum adsorption capacity of GO for CIPRO estimated by isotherm curve is about 250 mg/g of GO at the equilibrium time (24 hs) [47]. In our experimental conditions, the contact time at 5 mL/min is about 35 s, thus far from the equilibrium conditions, the maximum adsorption capacity expressed in mg removed/gr of total GO was 168 mg/g of GO (PSU-GO 3,5%), which is close to the value at the equilibrium (250 mg/g), this indicating that the flow rate does not significantly affect the total removal capacity of PSU-GO HFs filters.

3.3. Molecular weight cut-off (MWCO) and ultrafiltration of PSU-GO HFs

The MWCO of PSU-GO 3.5% HFs, taken as reference, was determined by fluorescent dextrane filtration experiments. Fluorescein isothiocyanate (FITC) dextranes of different MW were filtered over PSU and PSU-GO HFs in dead end in-out modality. The MWCO of HFs is conventionally defined as the MW of the molecule with 90% retention. Fig. 6a shows the trend of retention vs FITC-Dextrane MW and a MWCO of 15 kDa, and 62 kDa are estimated for PSU and PSU-GO 3.5% HFs, respectively, in line with the porometer determination (Table S1, ESI). Nevertheless, permeability of PSU and PSU-GO HFs (UF coefficient) were almost comparable. Indeed, ultrafiltration coefficients estimated by flowing pure water through the filters and measuring pressure and ultrafiltration rate, were similar, i.e. 7.6±1.0 (PSU) and 10.1±1.7 (PSU-GO) (Fig. 6b and also Fig. S6, ESI).

3.4. Removal of PFASs and heavy metals

Tap water (pH 7, 1L) spiked with a mixture of fourteen PFASs (0.5 µg/L each) of different molecular size (C_3–C_{13}, Fig. 6) and end-substitution (sulphonates or carboxylates) was filtered through PSU, PSU-GO HFs 3.5%, and GAC for comparison (details in ESI, Fig. S7). All modules showed higher removal toward long chain molecules (C_8–C_{13}). PSU-GO showed higher removal for sulphonated PFASs respect to carboxylate analogues of same length (i.e. C_6: 99% for PFHxS vs 79% for PFHpA, or C_4:35% for PFBS vs 4% for PFPeA). Fig. 7 shows the removal efficiencies normalized to the amount of adsorbing material in each module, expressed as mass of PFASs removed per gram of sorbent material. The adsorption capacity of PSU and PSU-GO HFs was significantly higher than that of GAC for almost all PFASs. The total amount of PFASs removed by PSU-GO 3.5% was up to seven times more efficient than GAC.

According to previous studies [48–51], the two most important factors driving PFASs adsorption are hydrophobic interactions and electrostatic interactions. Fig. 7c shows the trend of PFASs removal with *n*-octanol/water partition coefficient ($\log K_{OW}$) for PSU and PSU-GO 3.5% HFs. It can be seen how $\log K_{OW}$ grows linearly with PFASs molecular weight (Fig. S8, ESI).

It can be observed that PFASs with $\log K_{OW}$ in the range 4.5–6.5 are better removed by PSU-GO HFs than PSU HFs, and that the same removal is observed for $\log K_{OW}$ higher than 6.5. This effect emerges

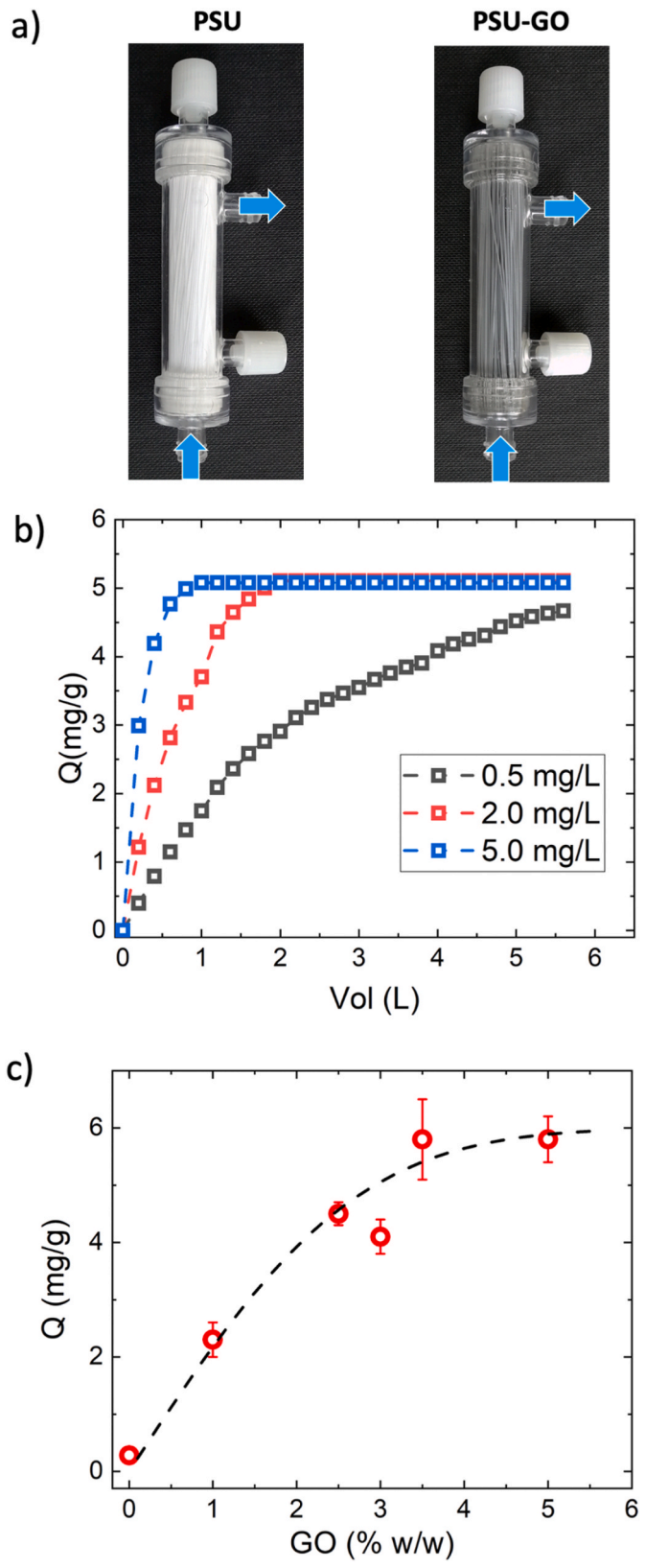

Fig. 5. a) From left to right, modules of PSU HFs, and PSU-GO 3.5% HFs. The arrow indicates water in and out pathways (i.e. dead end transmembrane in-out modality for PSU HFs and PSU-GO HFs,). b) Adsorption capacity as a function of the initial CIPRO concentration on PSU-GO 3.5% HFs. c) maximum adsorption capacity estimated by the loading curves (ESI), C_{IN}. CIPRO 5 mg/L, treated volume 3 L, flow rate 5 mL/min.

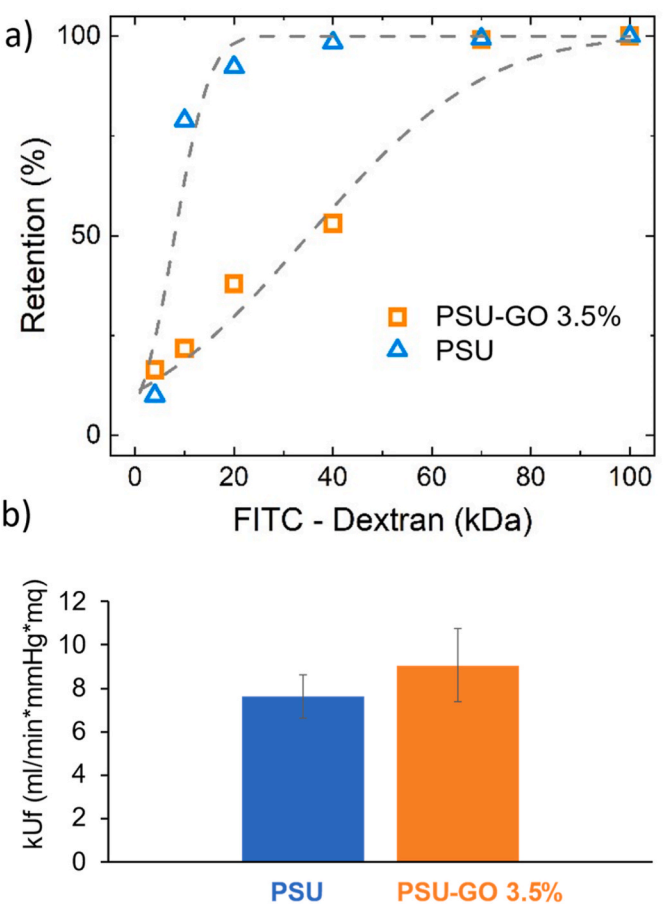

Fig. 6. Ultrafiltration range flow rate of PSU and PSU-GO 3.5% HFs. a) Retention of FITC-Dextran, b) Ultrafiltration coefficients of PSU and PSU-GO 3.5% HFs. Flow rate in shown in Fig. 6, ESI.

despite the higher hydrophilicity of PSU-GO with respect to PSU, as shown also by contact angle measurements (Fig. S3, ESI). The slightly higher hydrophilicity of PSU-GO seems particularly beneficial to the adsorption of short chain PFASs, ($4<\log K_{OW}<5$). Fig. 7c shows that in the $\log K_{OW}$ range 4.5-6-5, the higher is the hydrophilicity of the PFAS, the higher is the gap between the removal value for PSU and for PSU-GO HFs. This evidence suggests that repulsive electrostatic interactions are less relevant than hydrophobic interactions. On the other hand, experiments at higher PFASs initial concentration (10 μg/L rather than 0.5 μg/L; Fig. S9, ESI) show a significant drop in performance of PSU-GO HFs. At higher concentration, it has been shown that PFASs can aggregate into micelles [52], this would enhance the role of electrostatic rather than hydrophobic interactions as sorption driving forces. Overall, this evidence suggests a delicate interplay between hydrophobic and electrostatic interactions, which govern PFASs adsorption in this system. The overall proposed mechanism for PFASs adsorption in PSU-GO HFs modules is summarized in Fig. 10.

The removal of heavy metals and metalloids mix (As(V), Cd, Cr(III), Cu, Ni, Pb, U, and V) at 100 μg/L in mineral water (pH 7.5, see ESI, Table S4) was also tested. After treating 3 L of contaminated water, different affinities of metals towards the proposed materials were highlighted. The adsorption capacity of PSU, PSU-GO 3.5% HFs and GAC expressed as micrograms of contaminant removal normalized to gram of sorbent in the module, toward metal ions and metalloids is shown in Fig. 8. PSU-GO 3.5% HFs outperform GAC in the removal of Cr (III), Cu and Pb (see Fig. 8).

The plotting of removal efficiency vs treated volume (Fig. 9) shows that removal of Pb and Cu follows a similar trend, with initial removal capacity close to 100% for PSU-GO 3.5% HFs and final removal capacity

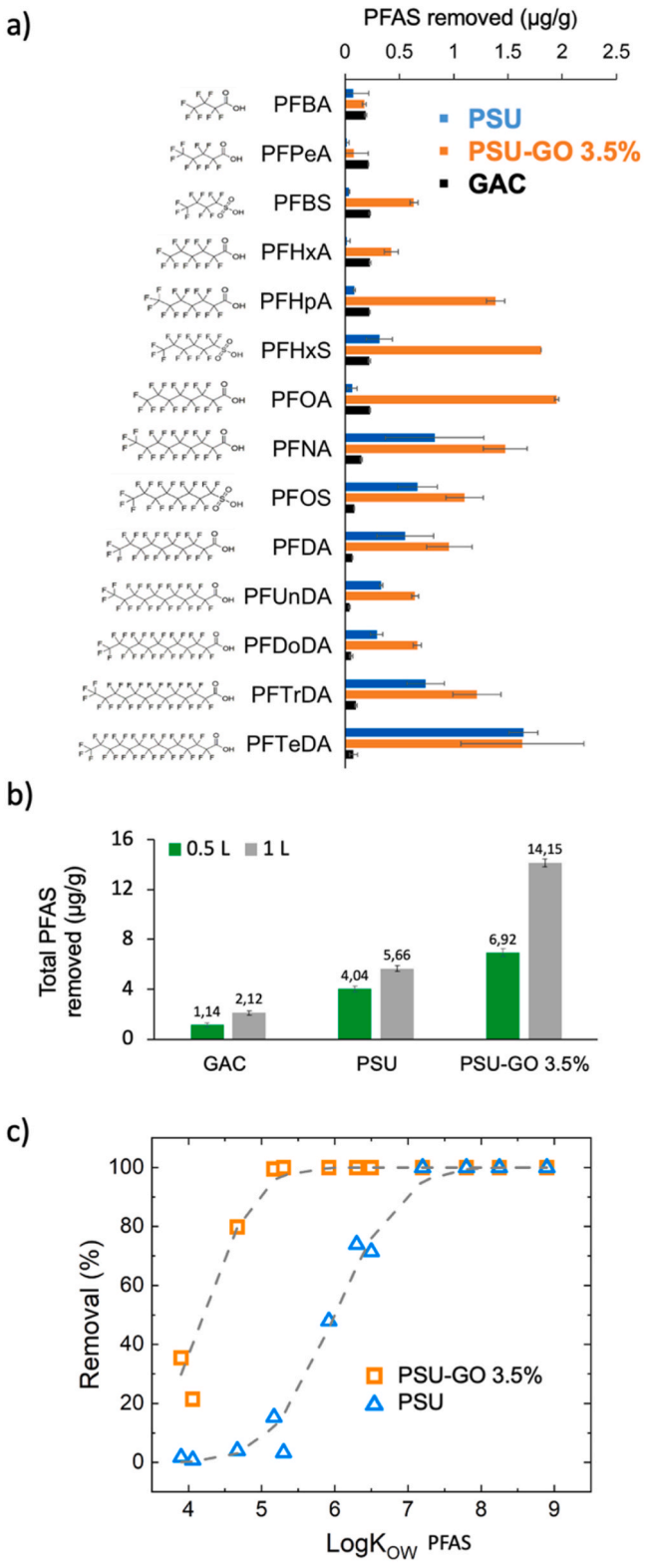

Fig. 7. a) Removal of a mixture of fourteen PFASs in tap water, total volume = 1 L, C_{IN} = 0.5 µg/L, flow rate = 5 mL/min in µg/g of PSU HFs (blue, total mass of composite 260 mg), PSU-GO 3.5% HFs (orange, total mass of composite 270 mg), and GAC (black, total mass 2.4 g). b) Total amount of PFASs removed µg/g after 0.5 L (green) and 1 L (grey) filtered. c) Removal of PFASs mixture in tap water vs the PFAS LogK_{OW} of PSU HFs (blue) and PSU-GO 3.5% HFs (orange). (For interpretation of the references to colour in this figure legend, the reader is referred to the Web version of this article.)

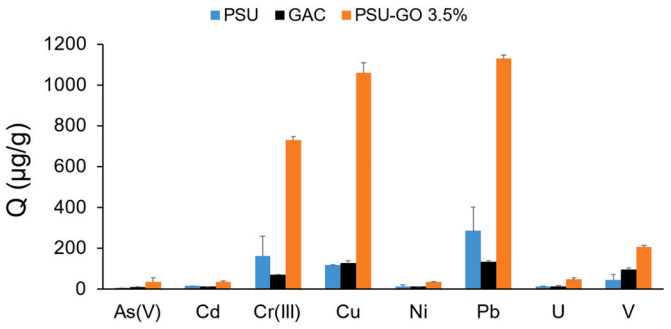

Fig. 8. Adsorption capacity Q (µg/g) towards a mixture of different heavy metals and metalloids. Three different adsorption materials were compared: PSU HFs (blue, left) and PSU-GO 3.5% HFs (orange, right), and GAC granules (black, middle). Flow rate 5 mL/min and total filtered volume 3 L, C_{IN} = 100 µg/L each. (For interpretation of the references to colour in this figure legend, the reader is referred to the Web version of this article.)

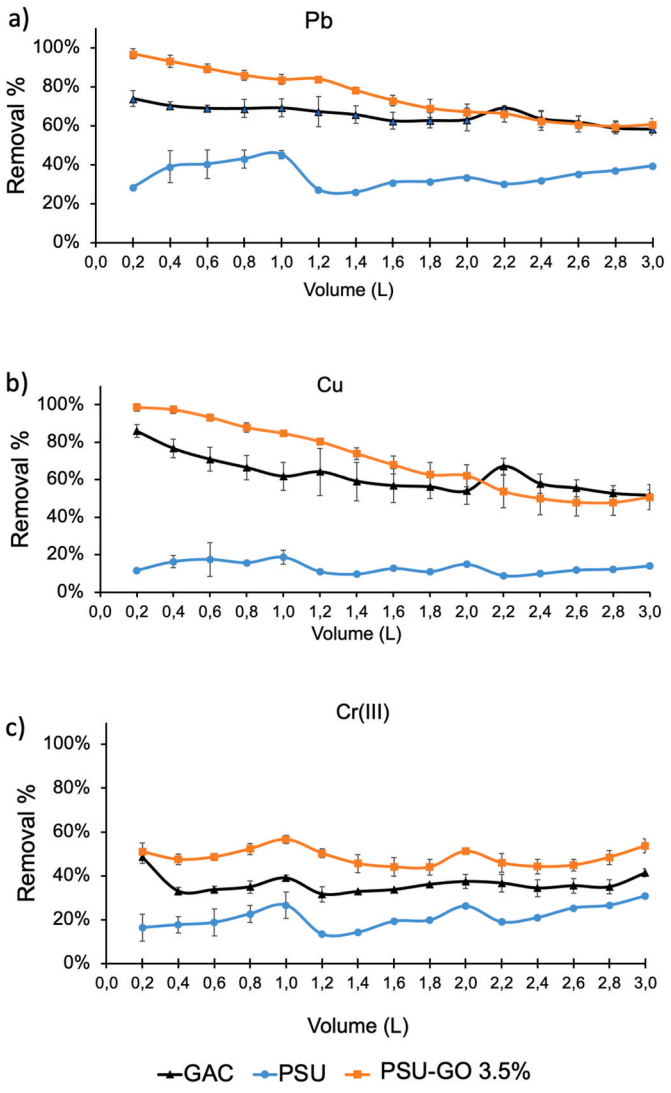

Fig. 9. Removal efficiency as function of treated volume (L) of a) Pb^{2+}, b) Cu^{2+}, c) $Cr(OH)_2^+/Cr(OH)^{2+}$.Three different adsorption materials were compared. PSU HFs (blue) and PSU-GO 3.5% HFs (orange) and GAC (black) granules. Flow rate 5 mL/min and total filtered volume 3 L. (For interpretation of the references to colour in this figure legend, the reader is referred to the Web version of this article.)

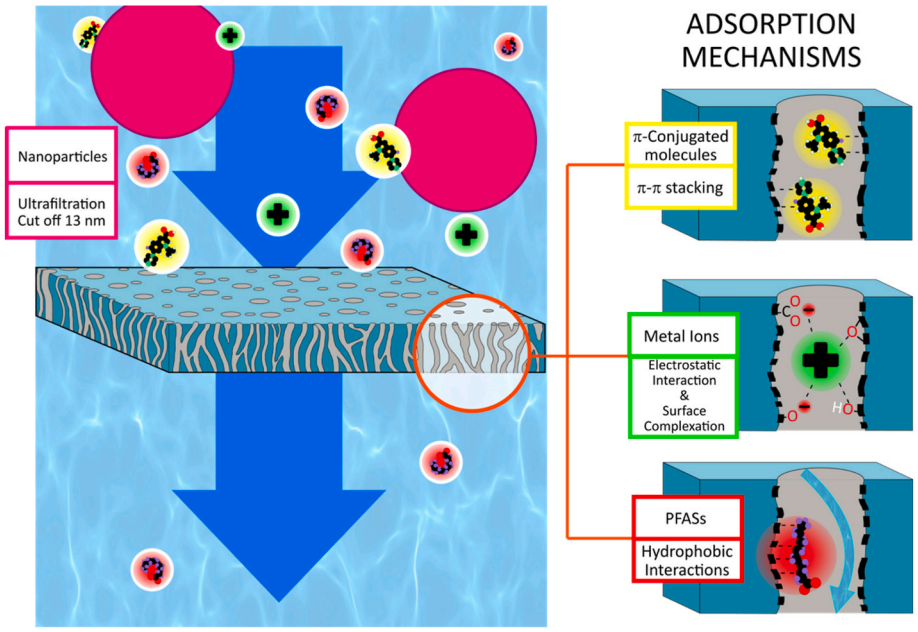

Fig. 10. Sketch of the adsorption mechanisms of pollutants on PSU-GO: π-conjugated molecules are adsorbed through π-π stacking, metal ions through electrostatic interactions and surface complexation, and PFASs through hydrophobic interactions.

of 50–60%. On the other hand, a constant removal of about 50% was observed for Cr(III). In the case of Pb and Cu, GAC removal capacity was about 10–20% lower for the first 2 L treated, then performance was similar to PSU-GO 3.5% HFs while negligible adsorption on neat PSU HFs was found for all the heavy metals and metalloids. The trend for remaining elements is reported in ESI (Fig. S10). Interestingly, as observed for ciprofloxacin removal, the observed PSU-GO HFs performances were independent on the flow rate (changing flow from 5 mL/min to 40 mL/min) as instead observed in the case of GAC (Fig. S12, ESI) whose removal became lower than 20%. In addition, by increasing flow rate in GAC filter a release of contaminants was observed demonstrating a labile adsorption of a fraction of them, due only to entrapment in GAC small pore more than chemical bonding. This was not observed operating with PSU-GO HF filters. Mobility of trapped metals was tested and compared among selected materials (one module for each material). As expected, the weakest adsorption was observed for PSU HFs, for which removal is likely to be governed just by pore trapping; while very low release was observed for Pb, Cu, and Cr(III) in both GAC and PSU-GO 3.5% HFs. The release of adsorbed metals was also tested, and details are reported in ESI (Fig. S13, Table S5).

Different studies proved higher Cu and Pb adsorption, if compared to other heavy metals, onto negatively charged surfaces with exposed –OH and –O groups as in our case, i.e. adsorption on GO, [53–57]. The adsorption passes through two different mechanisms: 1) exchange reaction onto permanent negatively charged sites, that involves not hydrolyzed cations; and 2) surface complexation at variable charged hydroxyl edges, that follows selective adsorption, according to the tendency of different metals to hydrolyze [54].

Cu and Pb hydrolyze more readily than Ni and Cd, and hence are more likely to interact with a hydroxylated surface, while Ni and Cd do not compete effectively for variable surface charges, due to their lower tendency to form hydrolysis products. Consequently, Ni and Cd adsorption is more restricted to permanent charge sites, especially in a competitive environment, such as a mix of metals. Previous studies [57–60] demonstrate that the overall metal affinities for goethite were generally found to follow the order Cr > Cu > Pb > Zn > Cd > Co > Ni > Mn > Ca > Mg, which was consistent with electronegativity or hydrated radii of the cations.

Overall, removal experiments on CIPRO, PFASs and metal ions

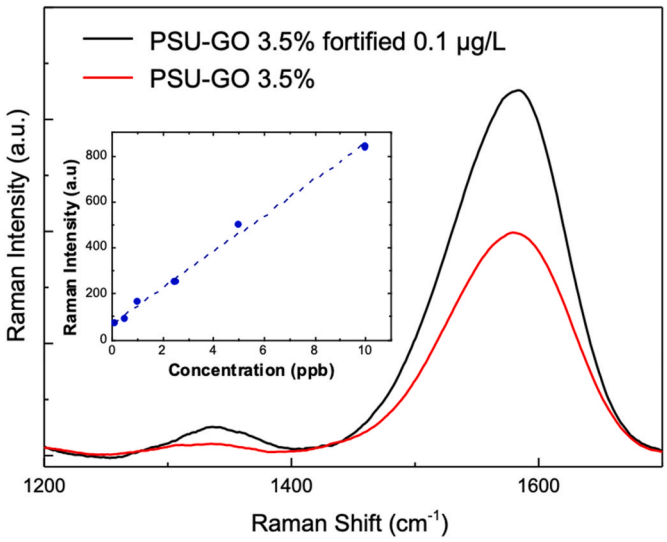

Fig. 11. SERS spectra for PSU-GO 3.5% (red) and PSU-GO 3.5% fortified 0.1 µg/L (black). The inset shows the calibration curve. (For interpretation of the references to colour in this figure legend, the reader is referred to the Web version of this article.)

suggest a removal mechanism based on the interplay of electrostatic interactions, hydrophobic interactions and π-π stacking between GO and the contaminants. Heavy metals are removed with higher performances than PFASs, likely thanks to the predominant surface complexation mechanisms favored also by positive electrostatic interaction with the negatively charged GO flakes. A schematic representation of adsorption mechanism for organics and heavy metals is depicted in Fig. 10.

3.5. Water potability and GO release test by surface-enhanced Raman spectroscopy (SERS)

Chemical and biological water potability was verified on tap water before and after filtration as listed in Table S6. In addition, to validate the safety of use of the PSU-GO HFs modules, we studied possible release

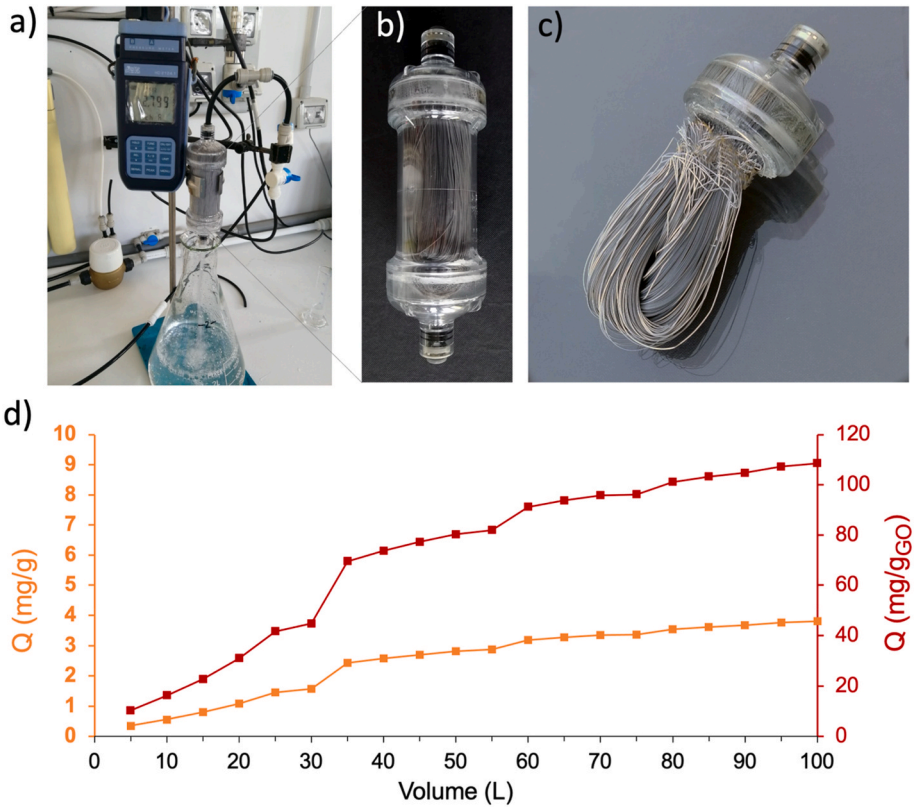

Fig. 12. a) PSU-GO 3.5% cartridge (FS 0,28 m^2, U-shaped HFs) connected at the tap (at 2.8 bar as shown by the manometer). Composite weight in each module about 6 g, with 210 mg of GO. b) zoom of the cartridge and c) of the U shape assembled fibers. d) Removal trend of CIPRO (spike at 1 mg/L).

of GO nanosheets during water purification. To this aim, we exploited a method, recently developed by some of us [46], able to detect and quantify GO in water samples at ultra-trace levels using surface-enhanced Raman spectroscopy (SERS). The methodology is based on the deposition of water GO dispersions on a SERS active substrate based on gold nanoparticles.

The optimized analytical protocol was applied to the detection and quantification of GO in tap water samples filtered through PSU HFs and PSU-GO 3.5% HFs modules. Water (1L) was filtered at a flow of 250 mL/min, i.e. 2.5-fold higher the maximum operating flow for PSU HFs prototype cartridges in Fig. 1b.

No significant differences can be found between the spectra of water samples filtered using PSU and PSU-GO 3.5% HFs modules (ESI, Fig. S15), indicating no GO release over the limit of detection (0.11 μg/L).

In order to further validate the measurements, one of the samples was fortified, i.e. GO was added to obtain a GO concentration of 0.1 μg/L and this new analyte was evaluated. Fig. 10 shows the spectra of the filtered sample as it and after fortification (Fig. 11). Our methodology predicted a concentration of 0.11 μg/L (in agreement with the experimental spike), with a relative standard deviation (RSD) below 4, in accordance with previously RSD of the method.

Fig. S15 (ESI) shows the spectra of water samples prepared by sonication of different quantities of PSU-GO in water (Fig. S15a) as well as the comparison to the SERS spectra of water samples prepared from sonication of PSU HFs as control sample (same amount, Fig. S15b). The sonication of PSU-GO fibers in water clearly causes the release of small quantities of GO and this release can be easily detected by our SERS protocol. Noteworthy, not significant differences between the results obtained with fibers extracted from new modules or modules already used for water filtration. Finally, considering a 3.5% of GO in PSU-GO HFs, the calculated release of GO after 30 min of sonication, was always lower than 0.2% (ESI, Table S8). To the best of our knowledge, this is the first case of study on release from PSU-graphene composite with a limit of quantification below the mg/L limit, typically achieved by UV–vis or TOC analyses [61].

3.6. Preliminary real conditions POU test

For validation of PSU-GO 3,5% HFs modules we performed a removal test in a pilot connected to the tap working with a reservoir allowing us to spike water before treatment with the PSU-GO modules. Module with U-shaped bundles (0.28 m^2 Fig. 12a and b) were produced since they are the standard POU module structure proposed by the producer (Medica spa). The amount of GO estimated in these modules was about 210 mg on a total HF weight of 6 g. For validation, tap water (100 L) was spiked with CIPRO (at 1 mg/L) and operated at about 2.5 bar (2 L/min). 5 L samples were collected and at each sampling the inlet solution was also collected and checked by HPLC-UV analysis. Fig. 11 shows the overall set-up (a) the module structure (b) and U-shape membranes inside the module (c). An initial removal of about 65% was found which decrease to about 30% after 40 L (Fig. S17, ESI). Despite the observed removal decay, the total mass of removed CIPRO in 100 L normalized to the amount of GO in the module, was about 110 mg removed per g of GO, compared to the 168 mg/g GO obtained in lab scale prototypes tested at 5 mL/min (Fig. S5, ESI). The estimated contact time of real size U-shaped module at 2 L/min is 10-fold lower than the one of lab scale prototypes tested at 5 mL/min, meaning that the removal of CIPRO by GO mediated adsorption is only partly affected by contact time (and/or flow rate).

It should be remarked that for this experiment we used a ppm spike of CIPRO which is far from the environmentally occurring concentration of CIPRO (ng-μg/L). This preliminary study on real size devices suggested that for POU applications, GO distribution and availability seem to affect the adsorption capacity more than flow rate. The removal decay could be likely enhanced by improving the distribution of GO

nanosheets within the composite and by reducing their aggregation which likely limits the exposed surface area and the overall adsorption.

4. Conclusions

A new class of GO enhanced ultrafiltration modules produced with a semi-industrial pilot plant, has been herein described. We demonstrated that PSU-GO HFs modules preserve ultrafiltration properties of commercial PSU HF modules, but also exhibited the adsorption properties typical of GO nanosheets. PSU-GO HFs have been proved superior to both pristine PSU HFs and GAC, the industrial standard adsorbent, in the removal of several classes of water contaminants. In particular, PSU-GO removal of ciprofloxacin antibiotic, Pb, Cu, and Cr(III); and perfluoroalkyl substances (PFASs, C4–C13) from real tap water matrix, were higher than that of GAC with a performance much less affected by the operational flow rate and negligible release at higher flow rate compared to for GAC. Higher selectivity for short chain PFASs with respect to GAC was observed. The importance of removing PFASs with $\log K_{OW}$ higher that 5 was pointed out by the Stockholm Convention on Persistent Organic Pollutants [62], since that value is the threshold for bio-accumulation and bio-concentration. Preliminary tests on POU real scale filters for tap water purification at tap operational conditions (pressure-flow rate) demonstrated comparable performance of small prototype working at low flow rate (5 mL/min) for CIPRO. Such capacity, as expected was lower than that of graphene nanosheets dispersion due to reaggregation of GO sheets in the composite. The absence of GO secondary contamination in after-treatment water has been verified through SERS experiments with a limit of detection of 0.1 μg/L and prove the safe use of these devices for water tretament. Some challenges are still to be tackled to exploit the full potential of this material, as compared to purely adsorption filters, to optimize the set-up to create more favorable kinetic conditions for the adsorption, to minimize the reaggregation of GO nanosheets to enhance their distribution and exposure of such sheets to the outer pore surface. Studies in these directions are currently in progress.

CRediT authorship contribution statement

Massimo Zambianchi: methodology, investigation. Sara Khaliha: methodology, investigation. Antonio Bianchi: visualization, writing – reviewing and editing. Francesca Tunioli: methodology, investigation, Alessandro Kovtun: investigation, formal analysis. Maria Luisa Navacchia: investigation, formal analysis. Anastasio Salatino: investigation. Barbara Casentini: methodology, investigation. Zhenyuan Xia: investigation. Davide Paci: investigation. Elena Briñas: investigation. Ester Vázquez: methodology, investigation. Vincenzo Palermo: conceptualization, validation. Letizia Bocchi: conceptualization, methodology, resources. Manuela Melucci: conceptualization, validation, writing – original draft.

Declaration of competing interest

The authors declare that they have no known competing financial interests or personal relationships that could have appeared to influence the work reported in this paper.

Acknowledgments

The authors gratefully acknowledge the support of this work by the project 881603- GrapheneCore3-H2020-SGA-FET- SH1 Graphil-GRAPHENE-FLAGSHIP and SH11 Saphegraph.

E. V. would like to thank the Spanish Ministerio de Ciencia e Innovación (project PID2020-113080RB-I00).

M.M. would like to thank Culligan® and MISTER Smart Innovation for the POU pilot installation at CNR.

Appendix A. Supplementary data

Supplementary data to this article can be found online at https://doi.org/10.1016/j.memsci.2022.120707.

References

[1] T.A. Tweddle, O. Kutowy, W.L. Thayer, S. Sourirajan, Polysulfone ultrafiltration membranes, Ind. Eng. Chem. Prod. Res. Dev. 22 (1983) 320–326.
[2] T. Sewerin, M.G. Elshof, S. Matencio, M. Boerrigter, J. Yu, J. de Grooth, Advances and applications of hollow fiber nanofiltration membranes: a review, Membranes 11 (2021) 890.
[3] M. Mondal, S. De, Treatment of textile plant effluent by hollow fiber nanofiltration membrane and multi-component steady state modeling, Chem. Eng. J. 285 (2016) 304–318.
[4] A.L. Ahmad, M. Sarif, S. Ismail, Development of an integrally skinned ultrafiltration membrane for wastewater treatment: effect of different formulations of PSf/NMP/PVP on flux and rejection, Desalination 179 (2005) 257–263.
[5] J. Gao, K.Y. Wang, T.-S. Chung, Design of nanofiltration (NF) hollow fiber membranes made from functionalized bore fluids containing polyethyleneimine (PEI) for heavy metal removal, J. Membr. Sci. 603 (2020), 118022.
[6] A. Abdelrasoul, H. Doan, A. Lohi, C.-H. Cheng, Morphology control of polysulfone membranes in filtration processes: a critical review, ChemBioEng Rev 2 (2015) 22–43.
[7] W.-P. Zhu, S.-P. Sun, J. Gao, F.-J. Fu, T.-S. Chung, Dual-layer polybenzimidazole/polyethersulfone (PBI/PES) nanofiltration (NF) hollow fiber membranes for heavy metals removal from wastewater, J. Membr. Sci. 456 (2014) 117–127.
[8] T.A. Otitoju, A.L. Ahmad, B.S. Ooi, Recent advances in hydrophilic modification and performance of polyethersulfone (PES) membrane via additive blending, RSC Adv. 8 (2018) 22710–22728.
[9] A. Pandele, O. Serbanescu, Ş.I. Voicu, Polysulfone composite membranes with carbonaceous structure. Synthesis and applications, Coatings 10 (2020) 609.
[10] S. Mangukiya, S. Prajapati, S. Kumar, V.K. Aswal, C.N. Murthy, Polysulfone-based composite membranes with functionalized carbon nanotubes show controlled porosity and enhanced electrical conductivity, J. Appl. Polym. Sci. 133 (2016).
[11] K. Matsumoto, T. Takahashi, S. Ishii, M. Jikei, Investigation of dispersibility of multi-walled carbon nanotubes using polysulfones with various structures, Int. J. Soc. Mater. Eng. Resour. 20 (2014) 77–81.
[12] M. Amini, M. Jahanshahi, A. Rahimpour, Synthesis of novel thin film nanocomposite (TFN) forward osmosis membranes using functionalized multi-walled carbon nanotubes, J. Membr. Sci. 435 (2013) 233–241.
[13] T. Hwang, J.-S. Oh, W. Yim, J.-D. Nam, C. Bae, H.-i. Kim, K.J. Kim, Ultrafiltration using graphene oxide surface-embedded polysulfone membranes, Separ. Purif. Technol. 166 (2016) 41–47.
[14] O. Kwon, Y. Choi, E. Choi, M. Kim, Y.C. Woo, D.W. Kim, Fabrication techniques for graphene oxide-based molecular separation membranes, Towards Industrial Application 11 (2021) 757.
[15] M. Ionita, A.M. Pandele, L. Crica, L. Pilan, Improving the thermal and mechanical properties of polysulfone by incorporation of graphene oxide, Composites Part B 59 (2014) 133–139.
[16] N. Meng, Z. Wang, Z.-X. Low, Y. Zhang, H. Wang, X. Zhang, Impact of trace graphene oxide in coagulation bath on morphology and performance of polysulfone ultrafiltration membrane, Separ. Purif. Technol. 147 (2015) 364–371.
[17] L. Liu, C. Tong, Y. He, Y. Zhao, C. Lü, Enhanced properties of quaternized graphenes reinforced polysulfone based composite anion exchange membranes for alkaline fuel cell, J. Membr. Sci. 487 (2015) 99–108.
[18] R. Rezaee, S. Nasseri, A.H. Mahvi, R. Nabizadeh, S.A. Mousavi, A. Rashidi, A. Jafari, S. Nazmara, Fabrication and characterization of a polysulfone-graphene oxide nanocomposite membrane for arsenate rejection from water, J. Environ. Health Sci. Engineer. 13 (2015) 61.
[19] Z.-Q. Huang, Z.-F. Cheng, Recent advances in adsorptive membranes for removal of harmful cations, J. Appl. Polym. Sci. 137 (2020), 48579.
[20] L. Qalyoubi, A. Al-Othman, S. Al-Asheh, Recent progress and challenges on adsorptive membranes for the removal of pollutants from wastewater. Part I: fundamentals and classification of membranes, Case Stud. Chem. Environ. Eng. 3 (2021), 100086.
[21] L. Badrinezhad, S. Ghasemi, Y. Azizian, A. Nematollahzadeh, Preparation and characterization of polysulfone/graphene oxide nanocomposite membranes for the separation of methylene blue from water, Polym. Bull. 75 (2018) 469–484.
[22] M. Zambianchi, M. Durso, A. Liscio, E. Treossi, C. Bettini, M.L. Capobianco, A. Aluigi, A. Kovtun, G. Ruani, F. Corticelli, M. Brucale, V. Palermo, M. L. Navacchia, M. Melucci, Graphene oxide doped polysulfone membrane adsorbers for the removal of organic contaminants from water, Chem. Eng. J. 326 (2017) 130–140.
[23] L. Jiang, Y. Liu, S. Liu, G. Zeng, X. Hu, X. Hu, Z. Guo, X. Tan, L. Wang, Z. Wu, Adsorption of estrogen contaminants by graphene nanomaterials under natural organic matter preloading: comparison to carbon nanotube, biochar, and activated carbon, Environ. Sci. Technol. 51 (2017) 6352–6359.
[24] B.S. Rathi, P.S. Kumar, P.-L. Show, A review on effective removal of emerging contaminants from aquatic systems: current trends and scope for further research, J. Hazard Mater. 409 (2021), 124413.
[25] R. Meffe, I. de Bustamante, Emerging organic contaminants in surface water and groundwater: a first overview of the situation in Italy, Sci. Total Environ. 481 (2014) 280–295.

[26] K.E. Murray, S.M. Thomas, A.A. Bodour, Prioritizing research for trace pollutants and emerging contaminants in the freshwater environment, Environ. Pollut. 158 (2010) 3462–3471.
[27] B. Petrie, R. Barden, B. Kasprzyk-Hordern, A review on emerging contaminants in wastewaters and the environment: current knowledge, understudied areas and recommendations for future monitoring, Water Res. 72 (2015) 3–27.
[28] R. Tröger, H. Ren, D. Yin, C. Postigo, P.D. Nguyen, C. Baduel, O. Golovko, F. Been, H. Joerss, M.R. Boleda, S. Polesello, M. Roncoroni, S. Taniyasu, F. Menger, L. Ahrens, F. Yin Lai, K. Wiberg, What's in the water? – target and suspect screening of contaminants of emerging concern in raw water and drinking water from Europe and Asia, Water Res. 198 (2021), 117099.
[29] E. Gagliano, M. Sgroi, P.P. Falciglia, F.G.A. Vagliasindi, P. Roccaro, Removal of poly- and perfluoroalkyl substances (PFAS) from water by adsorption: role of PFAS chain length, effect of organic matter and challenges in adsorbent regeneration, Water Res. 171 (2020), 115381.
[30] J. Glüge, M. Scheringer, I.T. Cousins, J.C. DeWitt, G. Goldenman, D. Herzke, R. Lohmann, C.A. Ng, X. Trier, Z. Wang, An overview of the uses of per- and polyfluoroalkyl substances (PFAS), Environ. Sci. J. Integr. Environ. Res.: Process. Impacts 22 (2020) 2345–2373.
[31] L. Liu, Y. Liu, B. Gao, R. Ji, C. Li, S. Wang, Removal of perfluorooctanoic acid (PFOA) and perfluorooctane sulfonate (PFOS) from water by carbonaceous nanomaterials: a review, Crit. Rev. Environ. Sci. Technol. 50 (2020) 2379–2414.
[32] P. McCleaf, S. Englund, A. Östlund, K. Lindegren, K. Wiberg, L. Ahrens, Removal efficiency of multiple poly- and perfluoroalkyl substances (PFASs) in drinking water using granular activated carbon (GAC) and anion exchange (AE) column tests, Water Res. 120 (2017) 77–87.
[33] N.B. Saleh, A. Khalid, Y. Tian, C. Ayres, I.V. Sabaraya, J. Pietari, D. Hanigan, I. Chowdhury, O.G. Apul, Removal of poly- and per-fluoroalkyl substances from aqueous systems by nano-enabled water treatment strategies, Environ. Sci. Water Res. Technol. 5 (2019) 198–208.
[34] S. Valsecchi, M. Rusconi, M. Mazzoni, G. Viviano, R. Pagnotta, C. Zaghi, G. Serrini, S. Polesello, Occurrence and sources of perfluoroalkyl acids in Italian river basins, Chemosphere 129 (2015) 126–134.
[35] V. Franke, P. McCleaf, K. Lindegren, L. Ahrens, Efficient removal of per- and polyfluoroalkyl substances (PFASs) in drinking water treatment: nanofiltration combined with active carbon or anion exchange, Environ. Sci. Water Res. Technol. 5 (2019) 1836–1843.
[36] D. Lu, S. Sha, J. Luo, Z. Huang, X. Zhang Jackie, Treatment train approaches for the remediation of per- and polyfluoroalkyl substances (PFAS): a critical review, J. Hazard Mater. 386 (2020), 121963.
[37] C.K. Pooi, H.Y. Ng, Review of low-cost point-of-use water treatment systems for developing communities, npj Clean Water 1 (2018) 11.
[38] M. Peter-Varbanets, C. Zurbrügg, C. Swartz, W. Pronk, Decentralized systems for potable water and the potential of membrane technology, Water Res. 43 (2009) 245–265.
[39] P. Westerhoff, P. Alvarez, Q. Li, J. Gardea-Torresdey, J. Zimmerman, Overcoming implementation barriers for nanotechnology in drinking water treatment, Environ. Sci.: Nano 3 (2016) 1241–1253.
[40] R. Mukherjee, S. De, Novel carbon-nanoparticle polysulfone hollow fiber mixed matrix ultrafiltration membrane: adsorptive removal of benzene, phenol and toluene from aqueous solution, Separ. Purif. Technol. 157 (2016) 229–240.
[41] K. Zahri, K.C. Wong, P.S. Goh, A.F. Ismail, Graphene oxide/polysulfone hollow fiber mixed matrix membranes for gas separation, RSC Adv. 6 (2016) 89130–89139.
[42] K. Sainath, A. Modi, J. Bellare, In-situ growth of zeolitic imidazolate framework-67 nanoparticles on polysulfone/graphene oxide hollow fiber membranes enhance CO2/CH4 separation, J. Membr. Sci. 614 (2020), 118506.
[43] https://eur-lex.europa.eu/legal-content/EN/TXT/?uri=CELEX%3A32020L2184, 2020 in.
[44] W. Peng, H. Li, Y. Liu, S. Song, A review on heavy metal ions adsorption from water by graphene oxide and its composites, J. Mol. Liq. 230 (2017) 496–504.
[45] S.Z.N. Ahmad, W.N. Wan Salleh, A.F. Ismail, N. Yusof, M.Z. Mohd Yusop, F. Aziz, Adsorptive removal of heavy metal ions using graphene-based nanomaterials: toxicity, roles of functional groups and mechanisms, Chemosphere 248 (2020), 126008.
[46] E. Briñas, V. Jehová González, M.A. Herrero, M. Zougagh, Á. Ríos, E. Vázquez, Submitted, 2022.
[47] S. Khaliha, T.D. Marforio, A. Kovtun, S. Mantovani, A. Bianchi, M. Luisa Navacchia, M. Zambianchi, L. Bocchi, N. Boulanger, A. Iakunkov, M. Calvaresi, A.V. Talyzin, V. Palermo, M. Melucci, Defective graphene nanosheets for drinking water purification: adsorption mechanism, performance, and recovery, FlatChem 29 (2021), 100283.
[48] M. Ateia, A. Maroli, N. Tharayil, T. Karanfil, The overlooked short- and ultrashort-chain poly- and perfluorinated substances: a review, Chemosphere 220 (2019) 866–882.
[49] C.T. Vu, T. Wu, Adsorption of short-chain perfluoroalkyl acids (PFAAs) from water/wastewater, Environ. Sci. Water Res. Technol. 6 (2020) 2958–2972.
[50] T. Jin, M. Peydayesh, R. Mezzenga, Membrane-based technologies for per- and poly-fluoroalkyl substances (PFASs) removal from water: removal mechanisms, applications, challenges and perspectives, Environ. Int. 157 (2021), 106876.
[51] T. Jin, M. Peydayesh, H. Joerss, J. Zhou, S. Bolisetty, R. Mezzenga, Amyloid fibril-based membranes for PFAS removal from water, Environ. Sci. Water Res. Technol. 7 (2021) 1873–1884.
[52] S. Kancharla, R. Jahan, D. Bedrov, M. Tsianou, P. Alexandridis, Role of chain length and electrolyte on the micellization of anionic fluorinated surfactants in water, Colloids Surf., A 628 (2021), 127313.
[53] L. de Pablo, M.L. Chávez, M. Abatal, Adsorption of heavy metals in acid to alkaline environments by montmorillonite and Ca-montmorillonite, Chem. Eng. J. 171 (2011) 1276–1286.
[54] P. Srivastava, B. Singh, M. Angove, Competitive adsorption behavior of heavy metals on kaolinite, J. Colloid Interface Sci. 290 (2005) 28–38.
[55] K. Lackovic, M.J. Angove, J.D. Wells, B.B. Johnson, Modeling the adsorption of Cd (II) onto Muloorina illite and related clay minerals, J. Colloid Interface Sci. 257 (2003) 31–40.
[56] M. Shi, X. Min, Y. Ke, Z. Lin, Z. Yang, S. Wang, N. Peng, X. Yan, S. Luo, J. Wu, Y. Wei, Recent progress in understanding the mechanism of heavy metals retention by iron (oxyhydr)oxides, Sci. Total Environ. 752 (2021), 141930.
[57] P. Trivedi, L. Axe, J. Dyer, Adsorption of metal ions onto goethite: single-adsorbate and competitive systems, Colloids Surf., A 191 (2001) 107–121.
[58] P. Zhang, J.-L. Gong, G.-M. Zeng, C.-H. Deng, H.-C. Yang, H.-Y. Liu, S.-Y. Huan, Cross-linking to prepare composite graphene oxide-framework membranes with high-flux for dyes and heavy metal ions removal, Chem. Eng. J. 322 (2017) 657–666.
[59] W.C. Chong, Y.L. Choo, C.H. Koo, Y.L. Pang, S.O. Lai, Adsorptive membranes for heavy metal removal – a mini review, AIP Conf. Proc. 2157 (2019), 020005.
[60] X. Wang, Z. Chen, S. Yang, Application of graphene oxides for the removal of Pb(II) ions from aqueous solutions: experimental and DFT calculation, J. Mol. Liq. 211 (2015) 957–964.
[61] A. Kovtun, A. Bianchi, M. Zambianchi, C. Bettini, F. Corticelli, G. Ruani, L. Bocchi, F. Stante, M. Gazzano, T.D. Marforio, M. Calvaresi, M. Minelli, M.L. Navacchia, V. Palermo, M. Melucci, Core–shell graphene oxide–polymer hollow fibers as water filters with enhanced performance and selectivity, Faraday Discuss 227 (2021) 274–290.
[62] H. Fiedler, R. Kallenborn, J.d. Boer, L.K. Sydnes, The Stockholm convention: a tool for the global regulation of persistent organic pollutants, Chem. Int. 41 (2019) 4–11.